



Synergism of co-delivered nanosized antioxidants displayed enhanced anticancer efficacy in human colon cancer cell lines



Lipika Ray ^{a,*}, Manish Kumar Pal ^a, Ratan Singh Ray ^{a,b}

^a CSIR-Indian Institute of Toxicology Research, P.O. Box No. 80, M.G. Marg, Lucknow, UP, 226001, India

^b Academy of Scientific and Innovative Research, New Delhi 110001, India

ARTICLE INFO

Article history:

Received 15 November 2016

Received in revised form

24 February 2017

Accepted 25 February 2017

Available online 6 March 2017

Keywords:

Chemoprevention

Therapeutic agent

Colon cancer

Synergistic effect

Apoptosis

ABSTRACT

Combination of chemopreventive and/or therapeutic agents is the imminent smart approach to cope up with cancer because it may act on multiple targets through different pathways. In the present study, we have synthesized multiple chemopreventive and/or therapeutic agents (Curcumin, Quercetin and Aspirin) loaded nanoparticles by simple cation-anion interaction among the amine groups of chitosan (CS) and phosphate groups of sodium hexametaphosphate (SHMP). These nanosized bioactive materials (CS-SHMP-CQA-NPs) were well characterized and found most effective in colon cancer cell line (HCT-116) compared to other cancer cell lines. Triplex chemopreventive and/or therapeutic agents-loaded NPs were synergistically inducing apoptosis in HCT-116 cells compared to two-chemopreventive agents-loaded NPs as evident by an increase in sub-G₁ cells (percent), and chromatin condensation along with the decrease in mitochondrial membrane potential (MMP). Interestingly, Chou–Talalay analysis revealed that CS-SHMP-CQA-NPs showed strong synergistic effect in its all doses. Thus, our study demonstrates that nanoparticles based bioactive materials significantly inhibit the growth of HCT-116 cells and thus could be a promising approach for colon cancer chemoprevention.

© 2017 The Authors. Production and hosting by Elsevier B.V. on behalf of KeAi Communications Co., Ltd. This is an open access article under the CC BY-NC-ND license (<http://creativecommons.org/licenses/by-nc-nd/4.0/>).

1. Introduction

Cancer is the most challenging and complicated disease nowadays [1–4]. Among all cancers, colorectal cancer is one of the main cause of death worldwide and second foremost cause of death in United States that affects both men and women [5–7]. Although the recent improvement of diagnostic equipments and therapeutic technologies has been able to reduce the mortality [8,9], the treatment of colorectal carcinoma remains complicated [10] due to undesired side effects, such as nephrotoxicity, ototoxicity [11] etc. from traditional chemotherapeutic agents. Therefore, there is an urgent need to search for chemopreventive agents [12–14] that would impede cancer initiation and progression [15]. However, given the complex etiology [16] of cancer, an individual chemopreventive

agent may not be sufficient to avert cancer [17]. Therefore, combination of chemopreventive agents targeting multiple pathways is required to achieve enhanced therapeutic effect. In addition, the selection of chemopreventive agents should be based on their high therapeutic index, less side effects and ease of administration.

Curcumin (Cur) and quercetin (Quer) are well known chemopreventive agents and exhibit anticancer activity by [18,19] modulating numerous intracellular signaling pathways associated with inflammation, cellular growth, invasion, mutagenesis, oncogene expression, cell cycle alteration, and apoptosis [20–26]. Cur also prevents chemically induced carcinogenesis in colon [27,28], forestomach [27] and skin [29,30] without any noticeable side effects [31,32]. Interesting to note that Cur is in clinical trial (Phase IIa) for the prevention of colorectal adenomas [33]. Quer also exhibits cancer cell specific anti-proliferative and apoptosis inducing effect leaving normal cells unaffected [34]. Mouat et al. [35] reported that Quer exerts chemoprotective action towards colon cancer cells (SW480). Advantageously, combination of Cur and Quer induces programmed cell death, such as apoptosis, when DNA damage cannot be successfully repaired [36]. On the other hand, aspirin (Acetylsalicylic acid), a member under the classification of

* Corresponding author. Present address: Pharmaceutics Division, CSIR-Central Drug Research Institute, Sector 10, Jankipuram Extension, Sitapur Road, Lucknow, UP, 226031, India.

E-mail address: lipikaray@gmail.com (L. Ray).

Peer review under responsibility of KeAi Communications Co., Ltd.

nonsteroidal anti-inflammatory drugs (NSAIDs), is known to reduce cancer cell progression [37–39] by generating several anti-inflammatory cytokines [40–42]. Recently, found the fact that NSAID drugs, mostly the cyclooxygenase (COX)-2 inhibitors, are the promising candidate for cancer prevention [40,43,44]. In case of growth and invasion of colon cancers, the concentration of prostaglandins, particularly the E₂ series (PGE₂), cyclooxygenase-2 (Cox-2), HGF receptor (c-Met-R), beta-catenin and epidermal growth factor receptor (EGFR) are increased [45]. However, so far, mixed reports are available regarding the use of aspirin (Asp) in colon cancer as a chemopreventive agent [46,47]. Thus, it is important to study the chemopreventive activities of Asp in colon cancer cells in detail.

Therefore, keeping all these in mind that Cur, Quer and Asp have anticancer activities with least side effects and different targets, we questioned whether the combination of Cur, Quer and Asp, could demonstrate synergistic chemopreventive and/or therapeutic effects in colon cancer cell lines. To the best of our knowledge, till date, no group has reported the combinatorial anticancer effect of Cur, Quer and Asp in colon cancer cells. However, the therapeutic efficacy of Cur as chemopreventive agent, either single or in combination, is jeopardized by its poor bioavailability which may be overcome by making it nanotized [48,49]. In addition, nanotization of triplex chemotherapeutic agents would improve circulation time through the enhanced permeability and retention (EPR) effect [50,51].

Chitosan (CS), a highly biocompatible and biodegradable matrix [52] was chosen as a nanocarrier to deliver the nanoparticles of triplex chemopreventive and/or therapeutic agents. CS has large number of free amine groups which were cross linked with sodium hexametaphosphate (SHMP) [53] to build CS-SHMP nanoconjugate through electrostatic interactions. Overall, all the three chemopreventive and/or therapeutic agents were entrapped inside the CS-SHMP nanoconjugate which formed self-assembled nanoparticles (CS-SHMP-CQA-NPs).

Herein, we demonstrate that co-delivery of Cur, Quer and Asp loaded chitosan-SHMP nanoconjugate exhibited synergistic chemopreventive and/or therapeutic effects through apoptosis in colon cancer cell lines (HCT-116). Although, Cur and Quer combination have been studied as a chemopreventive agent in gastric cancer (MGC-803) cells [36] but chemopreventive efficacy of the combination of Cur, Quer and Asp in encapsulated form is not reported hitherto.

2. Materials and methods

2.1. Chemicals

All the specified chemicals and reagents viz., chitosan (75% deacetylated), sodium hexametaphosphate (SHMP), curcumin (Cur), quercetin (Quer) and aspirin (Asp) were purchased from Sigma (Sigma St Louis, MO, USA) unless otherwise stated. Culture media, fetal bovine serum (FBS), antibiotics-antimycotic solution and trypsin-EDTA were purchased from Gibco BRL, USA. Plastic wares and culture wares used in the study were procured commercially from Nunc, Denmark. Milli Q water (deionized water, double distilled) was used in all the experiments.

2.2. Cell culture

Cell lines used in the study viz., human epidermoid carcinoma (A-431), human breast carcinoma (MCF-7), human colon carcinoma (HCT-116) and immortalized human keratinocyte (HaCaT) cell lines were initially procured from National Centre for Cell Sciences, Pune, India and since then have been maintained at, CSIR-Indian Institute

of Toxicology Research, Lucknow, India, following the standard protocols.

2.3. Preparation of curcumin, quercetin and aspirin loaded chitosan nanoparticles (CS-SHMP-CQA-NPs)(2)

Initially, CS was dissolved in acetic acid to give a final concentration of 1 mg/mL. The CS solution was adjusted to pH 5 with 2 M NaOH. Drug (Cur:Quer:Asp) ratios (w/w) were kept at 1:1:3.5. The drug ratios have been chosen by following Zhang et al. [36] (Cur and Quer ratio) and Zhou et al. [54] (Cur and Asp ratio) reports to obtain maximum therapeutic index and synergism. Cur and Quer were dissolved in ethanol (50 mL), each separately and Asp was dissolved in water (20 mL). Solution of Cur and Quer in ethanol was added drop wise into the chitosan solution, followed by Asp in water solution. After that, SHMP solution (0.133% w/v in purified water) [53] was added drop-wise into the chitosan solutions under constant magnetic stirring as the nanoparticles formed spontaneously. The above solution was stirred for 15 h at 25 ± 2 °C. Subsequently, the resulting solution was dialyzed against double distilled water with stirring for 24 h with the water being changed at least 6 times to remove unwanted materials. It has been found that 24 h was sufficient to remove unwanted materials in a controlled experiment. The dialyzed solution was lyophilized for 24 h to obtain yellow solid [CS-SHMP-CQA (2)]. Nanoparticles were stored at 4 °C under anhydrous conditions in dark till use.

Similarly, two-drug-loaded nanoparticles [Cur and Quer entrapped NP, CS-SHMP-CQ (1a); Quer and Asp entrapped NP, CS-SHMP-QA (1b); Cur and Asp entrapped NP, CS-SHMP-CA (1c)] were also prepared without altering drug ratios.

2.4. Characterization of the NPs

2.4.1. Percent yield

After achieving the constant weight, yield (%) of NPs was calculated by using the following formula:

$$\text{Yield (\%)} = \frac{\text{Weight of nanoparticle}}{\text{Weight of (drug + polymer)}} \times 100$$

2.4.2. Particle size measurement

The mean particle size and the polydispersity index (PDI) of 1a, 1b, 1c and 2 were determined by dynamic light scattering (DLS) technique employing a nominal 5 mW He-Ne laser operating at 633 nm wavelength. The freeze dried NP was dispersed in aqueous buffer and the size was measured. The measurements were carried out at 25 °C with the following settings: 10 measurements per sample; refractive indices of CS, 1.523; viscosity of water, 0.89 cP. The particle size was measured in triplicate.

2.5. Drug loading and entrapment efficiency

The drug loading and encapsulation efficiency were determined by analyzing the NPs spectrophotometrically using Lambda Bio 20 UV/VIS Spectrophotometer (Perkin Elmer, USA). The amount of Cur, Quer and Asp present in the nanoparticles was estimated as follows: a known amount of NPs (1 mg/mL) was dispersed in the mixture of double distilled water: ethanol (1:1) solution by stirring the sample vigorously and the absorbance of the solution was measured at 265, 373 and 426 nm for Asp, Quer and Cur, respectively, and the amount of drug present was calculated from a previously drawn calibration curve of concentration vs. absorbance with different known concentrations of the drugs. The percent drug

loading (%DL) and entrapment efficiency (%EE) were calculated using the formulas as given below. All the measurements were performed in triplicate.

$$\%DL = \frac{\text{Weight of drug in NPs}}{\text{Weight of NPs}} \times 100$$

$$\%EE = \frac{\text{Amount of drug present in the polymeric NPs}}{\text{Weight of drug used}} \times 100$$

2.6. Nanoparticle surface morphology

The surface morphology of the NPs was characterized using transmission electron microscopy (TEM) and scanning electron microscopy (SEM).

2.6.1. Transmission electron microscopy (TEM)

Briefly, a drop of aqueous solution of lyophilized powder (1 mg/mL) was placed on a TEM grid surface and a drop of 1% uranyl acetate was added to the surface of the Formvar-coated grid. After 1 min of incubation, excess fluid was removed and the grid surface was air dried at 25 ± 2 °C before being loaded into the microscope. The NPs were visualized under the transmission electron microscope (FEI Company, OR, USA) operated at 80 kV, attached to a Gatan Digital Micrograph (PA, USA).

2.6.2. Scanning electron microscopy (SEM)

The NPs were characterized for their shape, surface morphology, and particle size distribution by high-resolution field emission SEM (Quanta FEG 450, FEI, Netherlands). The sample was placed on a double-stick conducting carbon tape over an aluminum stub and coated with gold under an argon atmosphere by means of a sputter coater (SC 7620, mini sputter coater, Quorum Technology Ltd., UK). Samples were analyzed at an accelerating voltage of 10 kV and a working distance of 10 mm in a high-vacuum mode.

2.7. Evaluation of chemopreventive agents released from NPs

To determine the release profile of nanoparticles, a known quantity of the particles (~5 mg) was dispersed in 1 mL of phosphate buffered saline (PBS), at pH 7.4 and 6.5, and kept in the dialysis tube, which was suspended in 20 mL of PBS in a glass vial and the solution was stirred at $240 \times g$ at 37 °C. At pre-determined intervals of time, samples were collected (ca. 200 μ L) from the glass vial followed by spectroscopic analysis at 265 nm, 373 nm and 426 nm for Asp, Quer and Cur, respectively, using UV/VIS spectrophotometer. The same amount of fresh buffer was added to the glass vial and the release study was continued. The quantity of the released drug was then calculated using a previously drawn standard curve of the pure drugs in PBS.

2.8. Cell viability by MTT and NRU assays

The cytotoxicity of CS-SHMP-CQA-NPs was evaluated in the growing cultures of human epidermoid carcinoma (A-431), human breast carcinoma (MCF-7), human colon carcinoma (HCT-116) and immortalized human keratinocyte (HaCaT) cell lines by MTT assay. Furthermore, the alteration in cell viability (MTT assay) was performed for **1a**, **1b**, **1c** and **2** to estimate the therapeutic efficacies between two- and three-drug-loaded NPs. In addition, cell viability assay (MTT) was performed by different drug concentrations of two-drug-loaded NPs **1a**, **1b** and **1c** (Fig. S1). The cellular responses

by different drug concentrations of **2** were also assessed by MTT and NRU assays in HCT-116 cell lines. The cells were treated with various concentrations (0.3, 0.7 and 1.4 μ g/mL) of free Cur; (1.1, 2.8 and 5.5 μ g/mL) of free Quer; (0.3, 0.8 and 1.6 μ g/mL) of free Asp; free drug combination 1 [Cur (0.3 μ g/mL) + Quer (1.1 μ g/mL) + Asp (0.3 μ g/mL)]; free drug combination 2 [Cur (0.7 μ g/mL) + Quer (2.8 μ g/mL)+Asp (0.8 μ g/mL)]; free drug combination 3 [Cur (1.4 μ g/mL) + Quer (5.5 μ g/mL) + Asp (1.6 μ g/mL)]; (2, 5 and 10 μ g/mL) of CS-SHMP-CQA-NPs for a period of 48 h in HCT-116 cell lines. Specifically, 2, 5 and 10 μ g/mL doses of **2** contain (0.3, 0.7 and 1.4) μ g/mL of Cur; (1.1, 2.8 and 5.5) μ g/mL of Quer and (0.3, 0.8 and 1.6) μ g/mL of Asp, respectively.

Briefly, 1×10^4 cells/well were seeded in 96-well plates and allowed to adhere for 24 h. The medium was replaced and cells were washed with PBS. The cells were then incubated with drugs for a period of 48 h. After the completion of incubation period, cells were washed with PBS and the cells of different groups were processed for standard protocol for viz., tetrazolium bromide salt MTT assay (MTT), and neutral red uptake assay (NRU). The detailed protocols are given below:

MTT assay: In brief, cells (1×10^4) cell/well were seeded in 96-well plates and kept in CO₂ incubator for 24 h at 37 °C prior to experiment. The various treatments were given as per mentioned above and kept in incubator for 48 h and followed by MTT (5 mg/mL) was added with 200 μ L complete medium. The culture plates were washed twice with PBS and 200 μ L DMSO was added to each well and mixed well to dissolve the content. The absorbance was recorded at 530 nm by using multiwell micro plate reader (Fluostar Omega-BMG Labtech).

Neutral red uptake assay: Briefly, after treatment for 48 h, the culture well plates were allowed to incubate for 3 h in complete medium (DMEM F-12 HAM) containing Neutral Red (NR) dye (50 μ g/mL) followed by a quick wash with fixative (1% w/v CaCl₂; 0.5% v/v formaldehyde) to remove the unbounded dye. The accumulated dye was extracted with 50% ethanol containing 1% (v/v) acetic acid and plates were kept for 20 min on a shaker. The absorbance was recorded at 540 nm.

2.9. Analysis of interaction between curcumin, quercetin and aspirin

Compusyn software program (version 1.0), based on the Chou–Talalay method, was employed to determine the nature of interaction between the two-/three-agents. This method utilizes a multiple drug-effect equation derived from enzyme kinetics model in which the output is represented as combination indexes (CI). Compusyn software defines synergy as CI value less than 1. Based on CI values, the extent of synergism/antagonism may be determined [55]. In brief, CI values between 0.9 and 0.85 would suggest a slight synergy, whereas those in the range of 0.7 to 0.3 are indicative of clear synergistic interactions between the drugs/agents. On the other hand, CI values in the range of 0.9–1.1 suggest a near additive effect and values more than 1.1 indicate antagonism. We have determined CI values for all two- and three-drug-loaded NPs (**1a**, **1b**, **1c** and **2**). For detailed *in vitro* studies, the dose was selected considering both the therapeutic efficacy and extent of synergism. The synergistic doses of 5 and 10 μ g/mL for CS-SHMP-CQA-NPs showed below IC₅₀ value and were used for all *in vitro* experiments. Doses of free Cur, Quer and Asp were chosen according to their entrapment efficiencies in CS-SHMP-CQA-NPs (10 μ g/mL).

2.10. EB/AO morphology assay

For the determination of live, apoptotic and necrotic cells, assay was performed as described by Ribble et al. [56] Cocktail of EB and

AO (100 $\mu\text{g/mL}$) was prepared in phosphate-buffered saline. This assay is based on apoptosis induced characteristic nuclear condensation and fragmentation, whereas necrosis is characterized by the inability to exclude vital dye, leading to orange staining of nuclei. This procedure was used for qualitative analysis of apoptotic and necrotic cells after the treatment of (1.4 $\mu\text{g/mL}$) of free Cur; (5.5 $\mu\text{g/mL}$) of free Quer; (1.6 $\mu\text{g/mL}$) of free Asp; (5 and 10 $\mu\text{g/mL}$) of CS-SHMP-CQA-NPs and control, cells were incubated for 30 min with cocktail of EB/AO (100 mg/mL). Free drug treatments are chosen as per the drug content in the highest dose of CS-SHMP-CQA-NPs i.e. 10 $\mu\text{g/mL}$. The apoptosis/necrosis was observed by fluorescence images in upright microscope (Nikon Eclipse 80i equipped with Nikon DS-Ri1 12.7 megapixel camera, Japan). For each group, all cells in four image frames were analyzed using NIH ImageJ analysis software (USA) by following literature reports [57,58]. Green stained cells were counted as live cells and bright orange/red stained cells were counted as apoptotic/necrotic cells. Percent (%) apoptotic cells were measured for each group [57].

2.11. Mitochondrial membrane potential assay

2.11.1. JC-1 staining

Qualitative and quantitative change of MMP was measured by JC-1 stain (Sigma-Aldrich kit). In healthy cells, JC-1 forms J-aggregates which display strong fluorescent (red) intensity with excitation and emission at 560 and 595 nm, respectively. However, in apoptotic cells, JC-1 exists as monomers which show strong fluorescent (green) intensity with excitation and emission at 485 and 535 nm, respectively. Cells were exposed to (1.4 $\mu\text{g/mL}$) of free Cur; (5.5 $\mu\text{g/mL}$) of free Quer; (1.6 $\mu\text{g/mL}$) of free Asp; (5 and 10 $\mu\text{g/mL}$) of CS-SHMP-CQA-NPs for 24 h. Free drugs treatments are chosen as per the drug content in the highest dose of CS-SHMP-CQA-NPs i.e. 10 $\mu\text{g/mL}$. After treatment, cells were incubated with 5 μM JC-1 (ENZO life sciences) stain for 30 min at 37 $^{\circ}\text{C}$, washed and images were visualized by fluorescence microscope [59] (Nikon Eclipse 80i equipped with Nikon DS-Ri1 12.7 megapixel camera, Japan). Fluorescent intensity per cell in four image frames for each group was quantified using NIH ImageJ analysis software (USA) by following reports [60–63]. Mitochondrial depolarization in each group was quantified by calculating the ratio of red to green fluorescent intensity and was normalized to the control (red-to-green fluorescent ratio of control considered as 1) [62–64].

2.11.2. Mitotracker and DAPI staining

Changes in MMP were also examined by mitotracker/DAPI fluorescent dye; Life Technologies (M7512). Briefly, (1.4 $\mu\text{g/mL}$) of free Cur; (5.5 $\mu\text{g/mL}$) of free Quer; (1.6 $\mu\text{g/mL}$) of free Asp; (5 and 10 $\mu\text{g/mL}$) of CS-SHMP-CQA-NPs [free drugs treatments are chosen as per the drug content in the highest dose of CS-SHMP-CQA-NPs i.e. 10 $\mu\text{g/mL}$] treated cells were incubated with mitotracker (100 nM) for 15 min at 37 $^{\circ}\text{C}$ and then washed twice with pre-warmed PBS/DMEM. The cells were then fixed with 4% para-formaldehyde for 20 min, permeabilized in triton X-100 (0.1%) for 20 min and stained with DAPI (0.1 $\mu\text{g/mL}$) for 5 min at 37 $^{\circ}\text{C}$. After washing the cells with PBS three times, images were acquired by Leica TCS-SPE (Leica Microsystem Nusloch Germany) microscope [65]. Fluorescent intensity per cell in four image frames for each group was quantified using NIH ImageJ analysis software (USA) and percent (%) fluorescent intensity (red) was measured by following reported method [20].

2.12. Cell cycle analysis

Cells were treated with (1.4 $\mu\text{g/mL}$) of free Cur; (5.5 $\mu\text{g/mL}$) of free Quer; (1.6 $\mu\text{g/mL}$) of free Asp and (5 and 10 $\mu\text{g/mL}$) of **2** for 24 h

[free drugs treatments are chosen as per the drug content in the highest dose of CS-SHMP-CQA-NPs i.e. 10 $\mu\text{g/mL}$] and then cells were trypsinized and kept in 70% alcohol at 4 $^{\circ}\text{C}$ for 24 h followed by cells were centrifuged at 600 \times g for 10 min and washed with PBS. After washing, cells were re-suspended in PBS and cells were incubated with RNase (0.1 mg/mL) and 0.05% triton-X-100 for 30 min at 37 $^{\circ}\text{C}$. Finally, cells were stained with PI (50 $\mu\text{g/mL}$) and kept in the dark for 30 min prior to analysis. The altered DNA contents were determined by flow cytometer (Influx, BD, USA) with the help of Cell Quest program and Mod Fit software.

2.13. Statistical analysis

All the data expressed as mean \pm standard deviation (SD) were representative of at least three or four independent experiments. When comparing more than two mean values of groups, one-way analysis of variance (ANOVA) followed by Tukey's post hoc test using Prism software (GraphPad Software Inc., Version 3.0, CA, USA) was performed. P value less than 0.05 was considered as statistically significant.

3. Results and discussion

3.1. Synthesis and characterization of chemopreventive and/or therapeutic agents loaded nanoparticles

The physically cross linked NPs were synthesized by positive charge carrier deacetylated chitosan and negative charge carrier sodium hexametaphosphate. After addition of CS and SHMP in water at acidic pH (pH = 5), it is expected to form physically cross linked CS-SHMP polymer (Fig. 1A). Three different chemopreventive agents were entrapped inside the physically cross linked polymer to form self-assembled nanoparticle. Cur, Quer and Asp loaded NPs were prepared with a ratio (w/w) of Cur:Quer:Asp (1:1:3.5) [36,54] drug:polymer (1:10) [66] in double distilled water at 25 \pm 2 $^{\circ}\text{C}$ to achieve optimum therapeutic index. The yield of **2** was found to be ~55%. Cur, Quer and Asp loading in physically cross linked CS-SHMP-NPs (**2**) was obtained with encapsulation efficiency of ~14, 55 and 16% for Cur, Quer and Asp, respectively. The alteration in the drug ratios occurred after entrapment could be attributed to the dissimilar interactions between the drugs and polymer matrix which is literature precedence [67]. The percent drug loading (%DL) was 1.5, 6.2 and 6.5% for Cur, Quer and Asp, respectively, of the physically cross linked CS-SHMP weight. It was speculated that the drugs were accommodated in the pocket generated by physically cross linking with cationic CS and anionic SHMP (Fig. 1B).

We have also prepared all possible combination of two-drug-loaded nanoparticles [CS-SHMP-CQ (**1a**), CS-SHMP-QA (**1b**), and CS-SHMP-CA (**1c**)] by following similar procedures to compare therapeutic efficacies as well as synergism with three-drug-loaded NPs (**2**). In case of two-drug-entrapped NPs, yields were found to be 72%, 65% and 52% for **1a**, **1b**, and **1c**, respectively. Moreover, encapsulation efficiencies of drugs for **1a**, **1b**, and **1c** were listed in Fig. 2A.

3.2. Size measurements

Sizes of the synthesized nanoparticles are a prerequisite for its efficient entry inside the cell. The sizes of the NPs (**1a**, **1b**, **1c** and **2**) were determined by dynamic light scattering (DLS) and revealed hydrodynamic diameters from 92 to 128 nm for this series (Fig. 2A). The average diameter of **2** was found to be 92 nm (PDI = 0.12) by DLS (Fig. 2B), which showed no sign of aggregation. Moreover, the size and surface morphology of **2** were determined by transmission

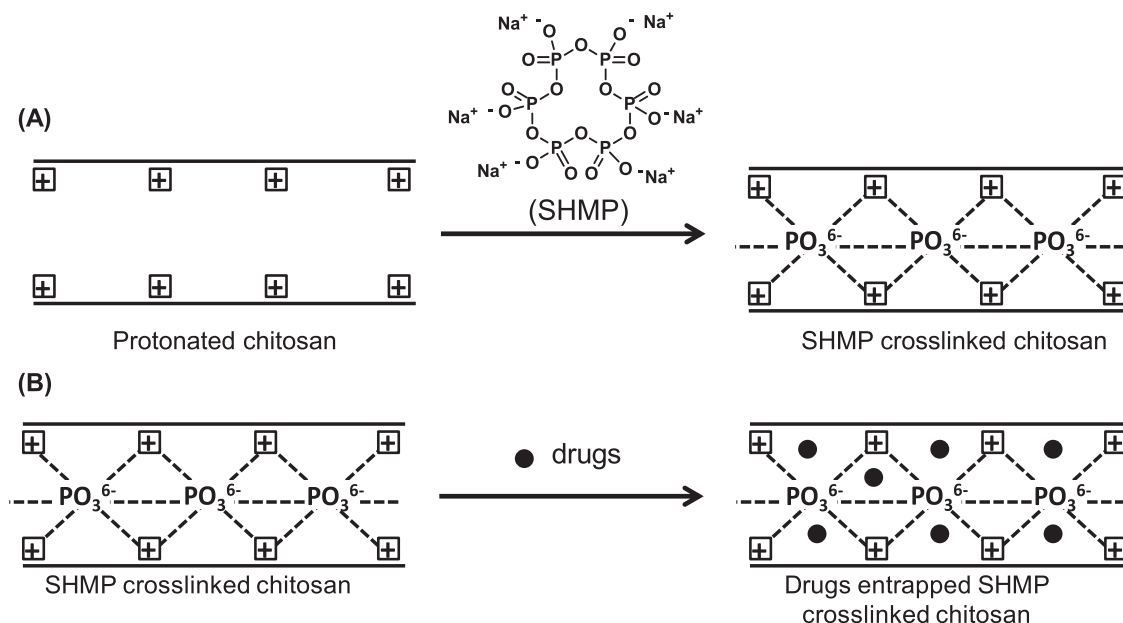


Fig. 1. Schematic diagram for the preparation of (A) SHMP cross linked chitosan (CS-SHMP) and (B) multiple drug loaded SHMP cross linked chitosan nanoparticles.

electron microscopy (TEM) (Fig. 2C) and scanning electron microscopy (SEM) (Fig. 2D), where **2** NPs were found to be almost spherical with size of 42–57 nm and 45–61 nm according to SEM and TEM, respectively. It is noteworthy that the particle size obtained by TEM and SEM are similar. However, the particle size determined by SEM and TEM was found to be significantly smaller than that measured by DLS measurements. This might be due to the fact that DLS measures hydrodynamic diameter of NPs, wherein, the amphiphilic NPs were surrounded by water molecules.

Moreover, chitosan has a tendency to swell in aqueous medium [68]. Conversely, SEM and TEM are used to measure the size of dehydrated NPs only. We deliberately kept the size of the NPs <150 nm assuming that smaller sized particles will have better cellular uptake and thereby would enhance efficiency of the anti-tumor drug. It is worth mentioning that the above sized NPs are adequate to reach the cancer cells, since the characteristic pore size cutoff of subcutaneously grown tumor ranges between 0.2 and 1.2 μm [66,69].

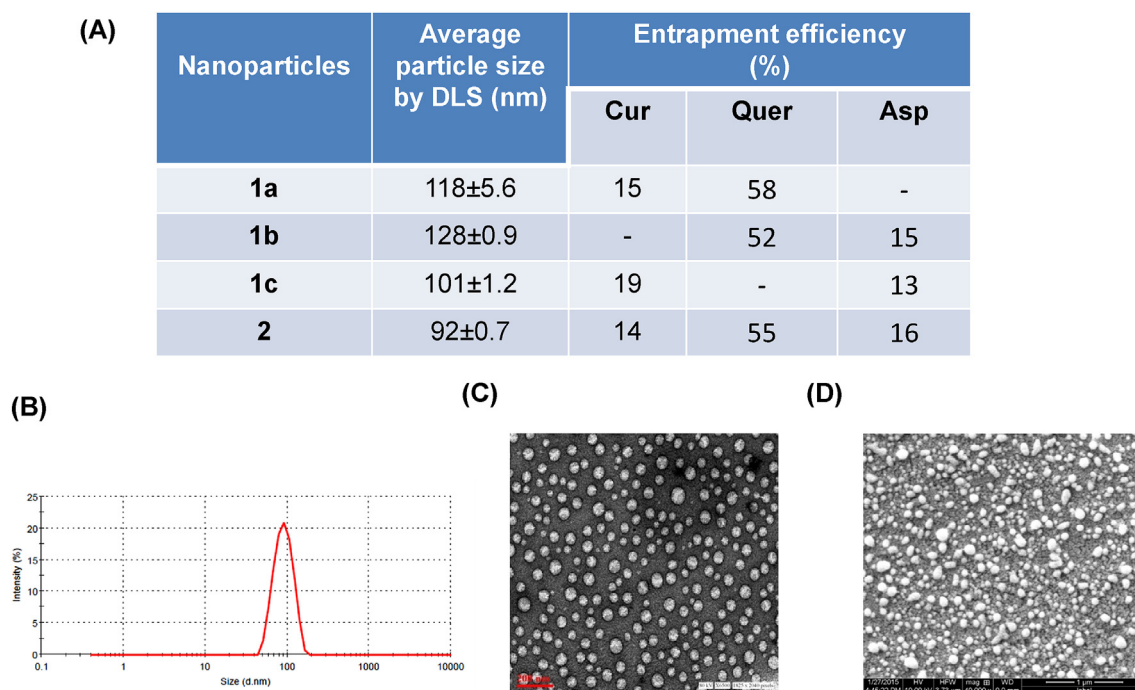


Fig. 2. Characterization of curcumin, quercetin and aspirin encapsulated CS-SHMP nanoparticles (A) Sizes by dynamic laser light scattering (DLS) and entrapment efficiencies of two- and three-drug-loaded nanoparticles (**1a**, **1b**, **1c** and **2**). (B) Representative picture of size distribution of **2** by DLS. (C) and (D) TEM and SEM images for **2**.

3.3. *In vitro* release profile of Cur, Quer and Asp loaded CS-SHMP-NPs

For designing an efficient NP-based drug delivery system, it is pertinent to characterize the retention and release properties of the drugs *in vivo*. To mimic the stability of chemopreventive agents loaded NPs in extracellular pH of normal tissues (*in vivo*); we carried out *in vitro* drug release study at the physiological pH (7.4). However, extracellular pH of most solid tumors is much lower than normal tissues and is ranging from pH 6.5 to 7.2. Thus, *in vitro* drug release study of **2** was also carried out at acidic pH (6.5). The release kinetics of all the three chemopreventive and/or therapeutic agents (Cur, Quer and Asp) from the NPs are the deciding factor for its efficient delivery at the site. For this, we examined the release pattern of **2** in PBS for 10 days at 37 °C (Fig. 3). Pattern of drugs release was slow and controlled [70], indicating its availability over a period of time. Drugs released from the NPs was found to be ~50, 20 and 60% at pH 7.4 and ~59, 25 and 66% at pH 6.5 for Cur, Quer and Asp, respectively, after 24 h followed by sustained release over an extended period of 7 days. Specifically, ~85, 92 and 99% of Cur, Quer and Asp, respectively, released from CS-SHMP-NPs after 7 days at pH 7.4. Interestingly, we found that the amount of drug release from **2** is faster at acidic pH than the physiological pH (7.4) (Fig. 3). It is believed that due to the presence of excess H⁺ ions the electrostatic interaction between CS and SHMP becomes weaker in acidic pH (6.5) compared to physiological pH (7.4). Therefore, it is expected that the release of drugs at the extracellular part of tumor would be high. These results indicate that **2** can be used as multiple drug carriers for antitumor activity.

3.4. Cell viability by MTT and NRU assays

To evaluate the anticancer effect of the combination of chemopreventive and/or therapeutic agents, cell viability assays were performed in HCT-116, A-431, MCF-7 and HaCaT cell lines. CS-SHMP-CQA-NP (**2**) efficiently reduced the cell viability in all cancer cell lines as IC₅₀ values are 2.2, 9.5, 12.2 and 55 µg/mL for HCT-116, A-431, MCF-7 and HaCaT cell lines, respectively (Fig. 4A). However, among all cancer cell lines, **2** showed significant and synergistic reduction of cell viability in HCT-116 compared to normal HaCaT cells. Therefore, we have performed

rest of the *in-vitro* studies in HCT-116 cell lines only. Moreover, to compare the therapeutic index and extent of synergism by two- and three-drug-loaded NPs, MTT assay was performed for **1a**, **1b**, **1c** and **2** in HCT-116 cell lines (Fig. 4B). Three-drug-loaded NPs (**2**) showed much lower IC₅₀ value ~ (2 ± 0.56 µg/mL) whereas two-drug-loaded NPs had IC₅₀ values of ~11 ± 1, 13 ± 0.6, and 18 ± 0.3 µg/mL for **1a**, **1b**, and **1c**, respectively. Therefore, three-drug-loaded NPs showed significant and synergistic reduction in HCT-116 cells compared to two-drug-loaded NPs (Fig. 4B, Fig. S1).

The alterations in cell viability were further performed with the treatment of Cur (0.3, 0.7 and 1.4 µg/mL), Quer (1.1, 2.8 and 5.5 µg/mL), Asp (0.3, 0.8 and 1.6 µg/mL), free drug combination 1 [Cur (0.3 µg/mL) + Quer (1.1 µg/mL) + Asp (0.3 µg/mL)], free drug combination 2 [Cur (0.7 µg/mL) + Quer (2.8 µg/mL) + Asp (0.8 µg/mL)], free drug combination 3 [Cur (1.4 µg/mL) + Quer (5.5 µg/mL) + Asp (1.6 µg/mL)] and CS-SHMP-CQA-NPs (**2**) (2, 5 and 10 µg/mL) in HCT-116 cell lines by MTT and NRU assays to estimate the anticancer effect of three-drug-loaded NPs. Specifically, 2, 5 and 10 µg/mL doses of **2** contain (0.3, 0.7 and 1.4) µg/mL of Cur; (1.1, 2.8 and 5.5) µg/mL of Quer and (0.3, 0.8 and 1.6) µg/mL of Asp, respectively. From cell viability assays, it was found that **2** (10 µg/mL) showed highest reduction in cell viability in HCT-116 cell lines after 48 h treatment. In HCT-116 cell lines, **2** (10 µg/mL) showed ~2.2, ~1.8 and ~2.3-fold reduction in cell viability than its corresponding free drugs concentrations, Cur (1.4 µg/mL), Quer (5.5 µg/mL) and Asp (1.6 µg/mL), respectively, in MTT assay. Interestingly, **2** (10 µg/mL) showed ~1.8-fold reduction in cell viability than its corresponding free drugs combination 3, [Cur (1.4 µg/mL) + Quer (5.5 µg/mL) + Asp (1.6 µg/mL)], in HCT-116 cell lines (Fig. 5A). Overall, the MTT assay revealed that the **2** (10 µg/mL) dose is the most effective and significant (p < 0.05) than all other doses including free drugs in combinations in HCT-116 cell lines. The free chemopreventive agent treatments are chosen as per the drug content in highest dose of **2** (10 µg/mL) in all other *in vitro* studies. The results obtained by NRU assay are similar as MTT assay in HCT-116 (Fig. 5A and B). Thus, from both the assays, it is important to note that the triplex chemopreventive/therapeutic agents in nanoparticles form showed most effective in colon cancer cell lines. Therefore, it may be speculated that combination of multiple chemopreventive and/or therapeutic agents in nano-

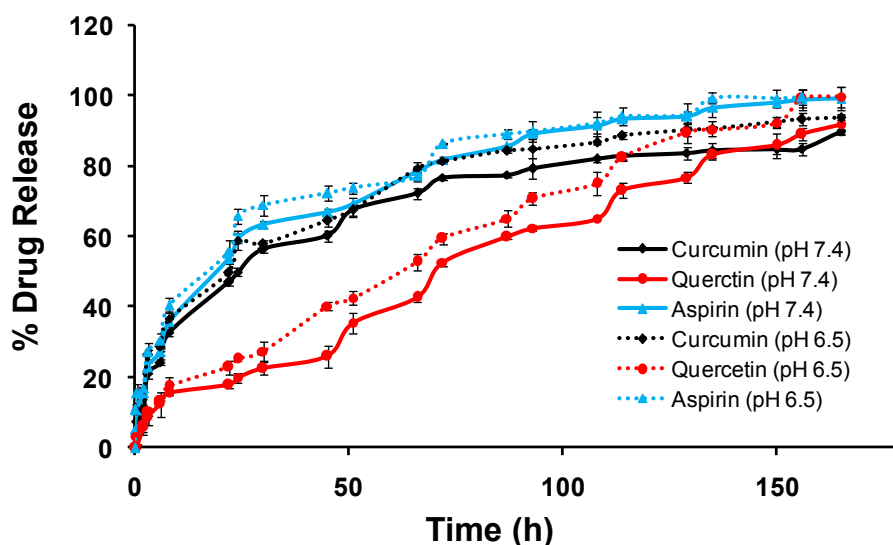


Fig. 3. *In vitro* release profile of Cur, Quer and Asp loaded NPs (**2**) at pH 7.4 and 6.5.

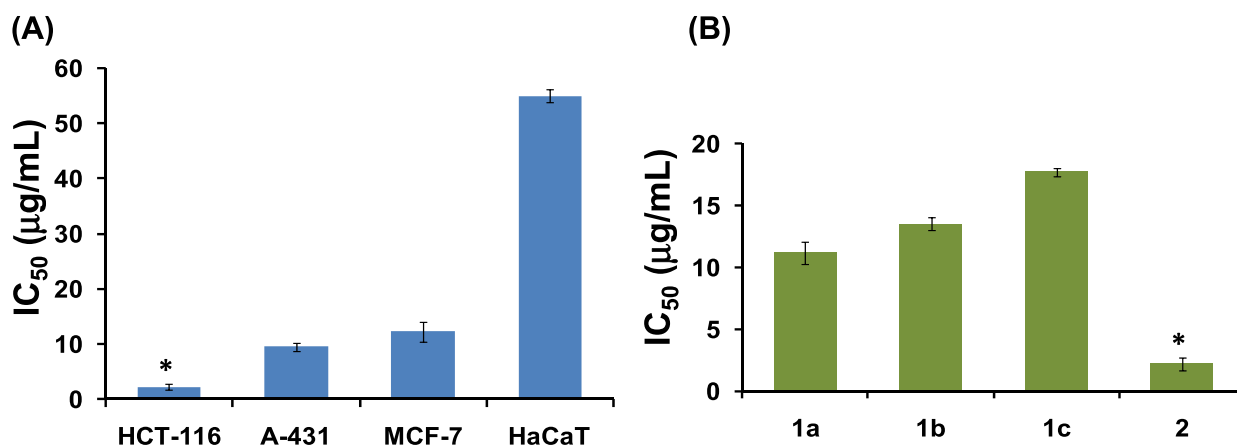


Fig. 4. (A) IC₅₀ values of CS-SHMP-CQA-NPs after 48 h of treatment on different cell lines [*P < 0.05 versus HaCaT]. (B) IC₅₀ values of two- and three-drug-loaded NPs (**1a**, **1b**, **1c** and **2**) in HCT-116 cell lines [*P < 0.05 versus **1a**, **1b**, and **1c**]. Three independent experimental data were summarized as mean ± SD.

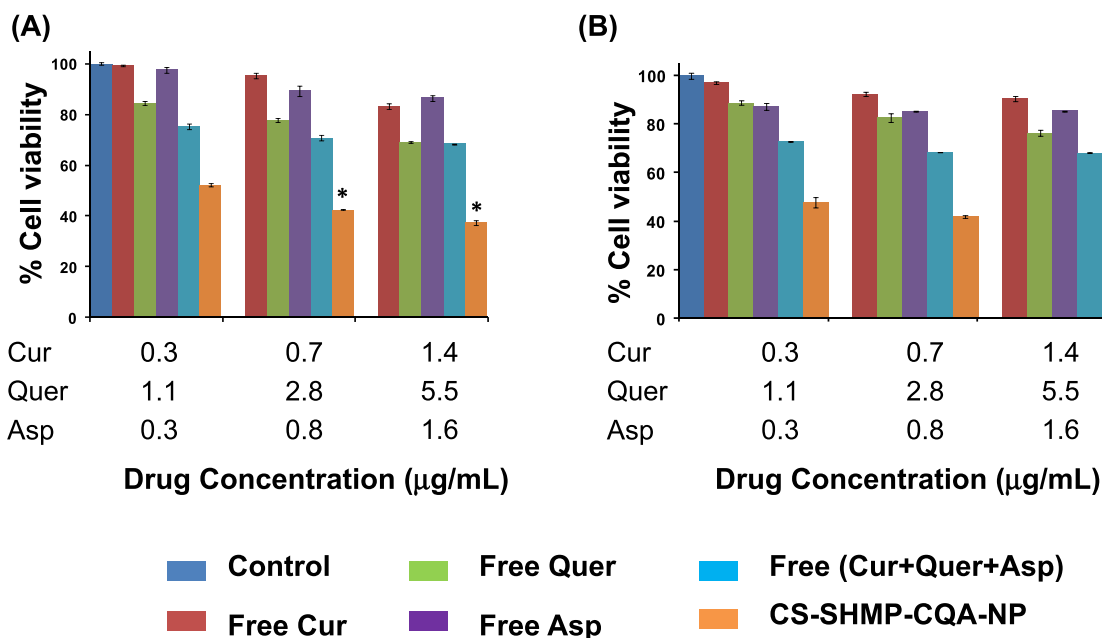


Fig. 5. Representative histogram of cell sensitivity of HCT-116 cells treated with free drugs, free drug combinations and triplex drug-loaded NPs by (A) MTT and (B) NRU assays. Three independent experimental data were summarized as mean ± SD. [*p < 0.05 versus control].

particulate form may show potential anticancer activity in *in vivo*.

3.5. Synergism

The combination of Cur, Quer and Asp in NP form causes a higher inhibition of growth in colon cancer cell lines (HCT-116) *in vitro* than either agent alone. The primary aim of this study is to evaluate whether combination of triplex chemopreventive agents in nanoparticle form would be a better therapeutic agent than the individual/combining form of free chemopreventive agents/two-drug-loaded NPs. Initially, the effects of free/combination of chemopreventive agents were evaluated in HCT-116 cell lines and then the data obtained from this study were plotted for the analysis of synergism by combination index (CI) method (Chou–Talalay method) [55]. Both, MTT and NRU data revealed that the triplex chemopreventive/therapeutic agents in the

nanoparticle form (**2**) showed a dose dependent and greater cell reduction than not only the drugs alone but two-drug-entrapped NPs (**1a**, **1b**, and **1c**) also (Figs. 4B and 5A & B and Fig. S1). The combination index (CI) for **2** (2, 5 and 10 µg/mL) treatment was found to be below 1; CI = 0.19, 0.33 and 0.56, respectively, suggests that the combination of chemopreventive agents as a NP interacts synergistically (Table 1 and Fig. 6D). However, two-drug-loaded NPs showed much higher CI values, thus indicated less synergism in all doses (Table 1 and Fig. 6A–C). None of two-drug-entrapped NPs, except CS-SHMP-CQ (CI = 0.97; slight synergism/additive effect), showed synergistic effect in HCT-116 cell lines which is also apparent from cell viability responses by different concentrations of two-drug-loaded NPs (**1a**, **1b**, and **1c**) (Fig. S1). Therefore, it is evident that three-drug-loaded NPs are more effective to inhibit colon cancer in HCT-116 cell lines than two-drug-loaded NPs. Hence, triplex chemopreventive/therapeutic agents loaded nanoparticles (CS-SHMP-CQA-NPs)

Table 1
Cell fraction affected at different doses of **1a**, **1b**, **1c**, and **2** and their corresponding CI values in HCT-116 cells.

Nanoparticles		Dose ($\mu\text{g/mL}$)	Fraction affected (Fa)	Combination Index (CI)
Two-drug-loaded NPs	1a	2	0.10	2.68825
		5	0.28	0.97555
		10	0.35	1.27262
	1b	2	0.15	1.23156
		5	0.25	1.12392
		10	0.32	1.30281
	1c	2	0.05	1.01313
		5	0.11	1.36611
		10	0.28	1.22575
Three-drug-loaded NPs	2	2	0.479	0.19304
		5	0.575	0.33455
		10	0.627	0.55627

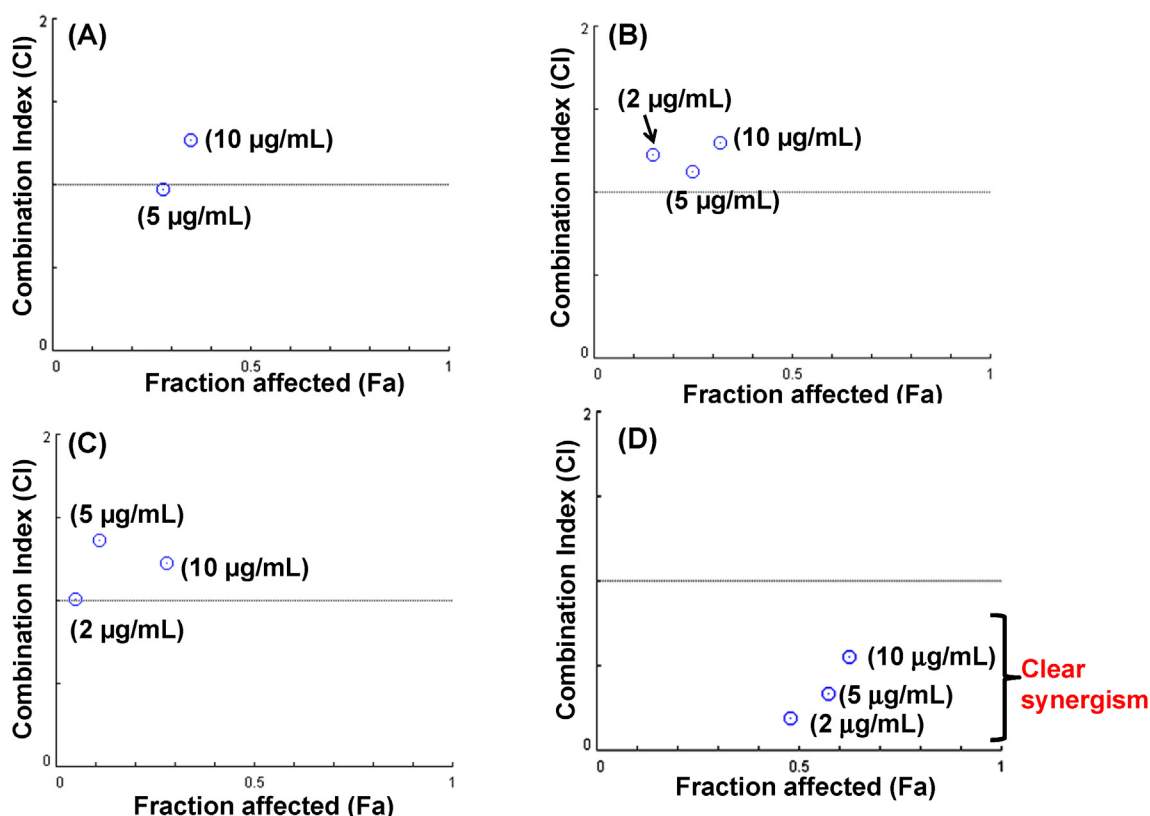


Fig. 6. Combination index (CI)–fraction affected (Fa) plot of two-drug-loaded NPs (**1a**, **1b**, and **1c**) and three-drug-loaded NPs (**2**) at 2, 5 and 10 $\mu\text{g/mL}$ doses in HCT-116 cells: (A) **1a**; (B) **1b**; (C) **1c**; (D) **2**. Generally, a CI < 1 indicates synergism between the drugs, a CI < 0.3 indicates strong synergy, CI = 1 indicates additive effect and CI > 1 indicates antagonistic effect.

are only considered for rest of *in vitro* studies. Furthermore, CS-SHMP-CQA-NPs (5 and 10 $\mu\text{g/mL}$) were selected as doses for all studies considering both the therapeutic efficacy and extent of synergism. However, CS-SHMP-CQA-NPs (10 $\mu\text{g/mL}$) found to be most effective dose for *in vitro* studies with strong synergism.

3.6. Cur, Quer and Asp loaded CS-SHMP-NPs induced apoptosis

Apoptosis is the vital cellular process by which many drugs induce cell-cycle arrest at sub- G_1 phase and thus destroy tumor cells [71]. The apoptosis inducing potential of CS-SHMP-CQA-NPs was examined by analyzing percent (%) cells with sub- G_0/G_1 DNA content. Particularly, the flow-cytometric analysis demonstrates that a significant shift ($p < 0.05$) in G_0/G_1 phase in **2** treated

HCT-116 cells compared to control and free drugs treated cells (Fig. 7). Specifically, **2** (10 $\mu\text{g/mL}$) treated HCT-116 cells showed ~1.7 fold higher number of cells with sub-diploid DNA content than Cur and Quer treated cells. However, cell cycle arrest at sub- G_1 phase in **2** (10 $\mu\text{g/mL}$) treated cells is ~6.1-fold more than Asp treated cells.

The cell cycle arrest in G_0/G_1 phase is indicating the progression of apoptosis. Cur, Quer and Asp loaded CS-SHMP-NP mediated apoptosis/necrosis was further established by ethidium bromide and acridine orange (EB/AO) morphological assay (Fig. 8A and B). Viable cells showed green fluorescence, while early, late apoptotic and necrotic cells showed several yellow-orange and red DNA (Fig. 8A). Control and Asp (1.6 $\mu\text{g/mL}$) treated cells showed normal morphology, however, Cur (1.4 $\mu\text{g/mL}$), Quer (5.5 $\mu\text{g/mL}$), NP (5 $\mu\text{g/mL}$) and NP (10 $\mu\text{g/mL}$) treated cells showed increase in number of

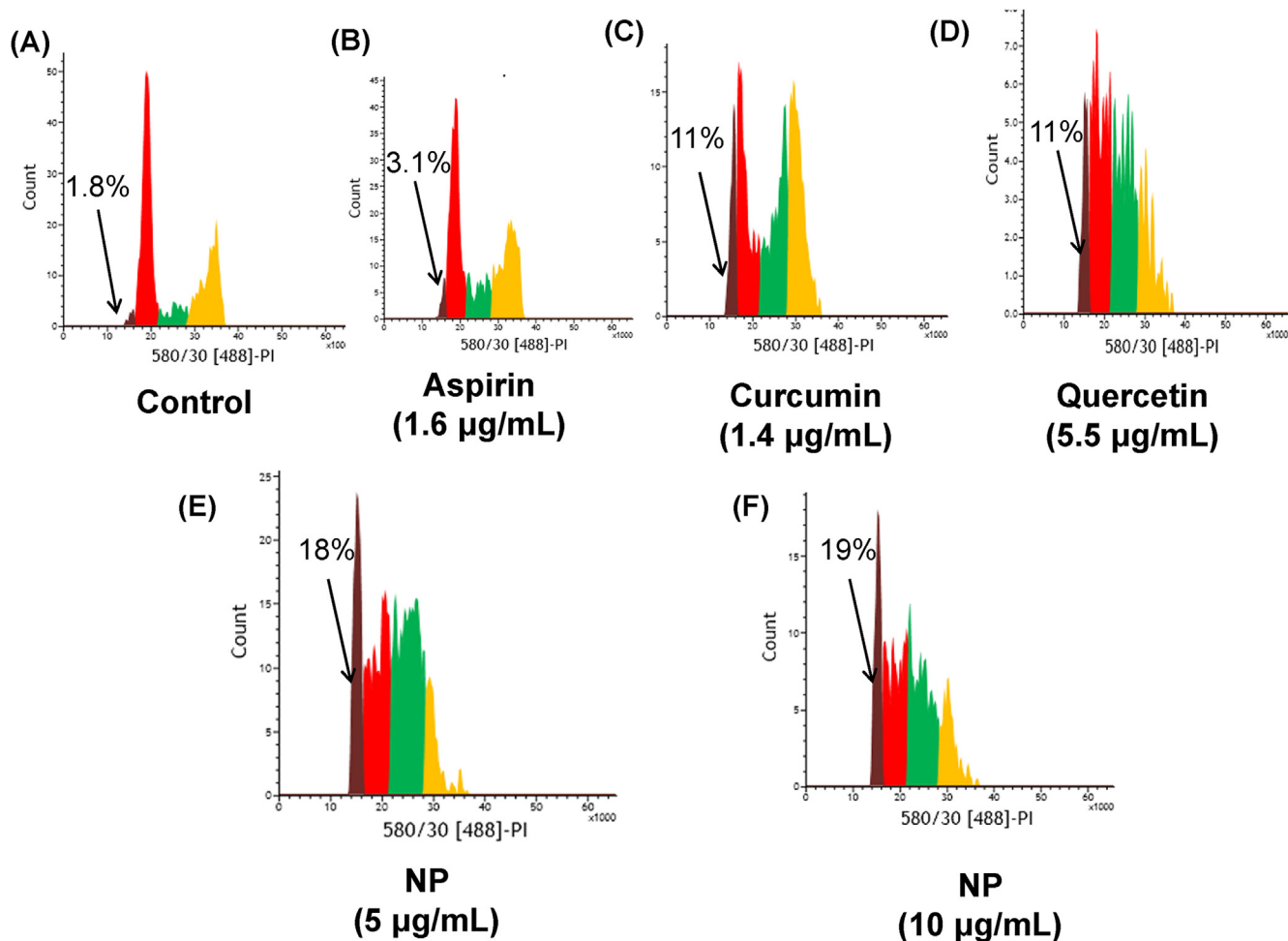


Fig. 7. Flow cytometric analysis of HCT-116 cells with sub- G_1 DNA content in (A) Control, (B) Aspirin (1.6 $\mu\text{g/mL}$), (C) Curcumin (1.4 $\mu\text{g/mL}$), (D) Quercetin (5.5 $\mu\text{g/mL}$), (E) CS-SHMP-CQA-NP (5 $\mu\text{g/mL}$), and (F) CS-SHMP-CQA-NP (10 $\mu\text{g/mL}$). Data represented as mean \pm SD of three independent experiments.

apoptotic cells and necrotic cells. Among them NP (10 $\mu\text{g/mL}$) treated cells showed maximum number of apoptotic/necrotic cells. The staining images for each group were analyzed by NIH ImageJ software (USA) [57,58]. Fig. 8B is clearly depicted that **2** induced significant cell damages/cell death in comparison to free drugs exposed cells. The percent (%) apoptotic cells indicated that CS-SHMP-CQA-NP (10 $\mu\text{g/mL}$) showed ~ 2 , ~ 1.4 , ~ 3 and ~ 1.4 -fold more apoptotic/necrotic cells compared to control, Asp (1.6 $\mu\text{g/mL}$), Cur (1.4 $\mu\text{g/mL}$) and Quer (5.5 $\mu\text{g/mL}$) treated cells, respectively (Fig. 8B). The data are in well co-ordination with cytotoxicity assays (MTT and NRU). Overall, data revealed that synergistically interacted triplex combination of chemopreventive and/or therapeutic agents in nanoparticle form showed more apoptotic/necrotic cells than the free drugs.

3.7. Mitochondrial membrane potential (MMP)

Mitochondrial dysfunction is a key feature of cells undergoing apoptosis [72]. Therefore, mitochondrial membrane potential (MMP, $\Delta\psi_m$) was detected by a MMP sensitive fluorescent dye JC-1. Monomer JC-1, displays green fluorescence with excitation and emission at 485 and 535 nm, accumulates in the mitochondrial matrix under the condition of high mitochondrial membrane potential of healthy cells where it forms JC-1 aggregates which show red fluorescence with excitation and emission at 560 and 595 nm. However, in apoptotic cells, JC-1 remains as monomer form due to

mitochondrial dysfunction under the condition of low mitochondrial membrane potential [64]. Thus, mitochondrial membrane depolarization can be measured by the extent of red to green fluorescence shift. The fluorescent images of mitochondria showed red fluorescence in control and free drugs treated cells, showing active mitochondria, but CS-SHMP-CQA-NPs showed dose dependent enhancement in green fluorescence with decreased mitochondrial activity (Fig. 9A). Therefore, the exposure of CS-SHMP-CQA-NP (**2**) showed significant red to green shift in fluorescence of JC-1 dye compared to control and free drug treatments. These results suggested that the increased amount of JC-1 aggregates was accumulated in CS-SHMP-CQA-NP (**2**) treated groups. Thus, mitochondrial membrane integrity is lost by inducing depolarization of mitochondrial membrane potential by CS-SHMP-CQA-NP. Fluorescence intensity was quantified in each group using NIH analysis software (USA) [60–63], and the ratio of red to green fluorescence intensity was calculated [62–64] which is clearly depicted that triplex chemopreventive agents loaded CS-SHMP-CQA-NPs synergistically induced ~ 3 , ~ 2.6 , ~ 1.4 and ~ 1.1 fold loss of membrane potential in comparison to control, Asp (1.6 $\mu\text{g/mL}$), Cur (1.4 $\mu\text{g/mL}$), and Quer (5.5 $\mu\text{g/mL}$), respectively, (Fig. 9B).

The DNA damage and reduced mitochondrial membrane potential in case of triplex drug-loaded NPs (**2**) were analyzed by mitotracker/DAPI staining and also confirmed that the prominent formation of chromatin condensation in case of **2** treated cells (Fig. 10A). The quantitative analysis of mitotracker/DAPI staining for

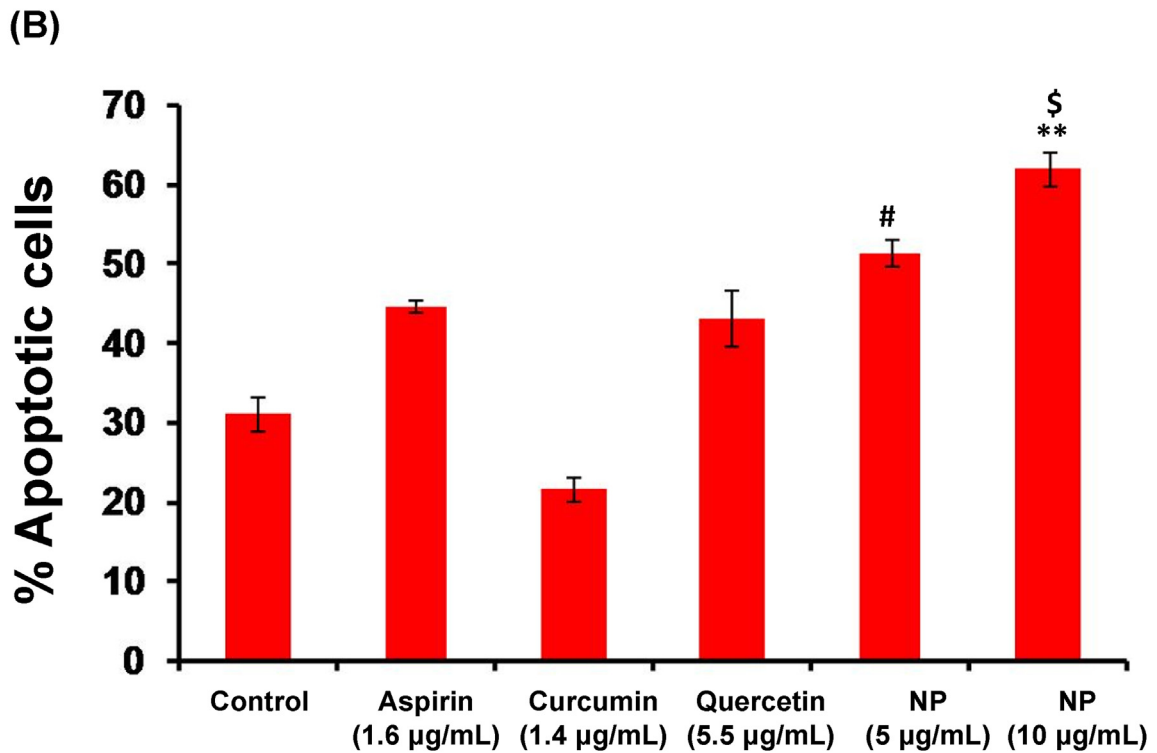
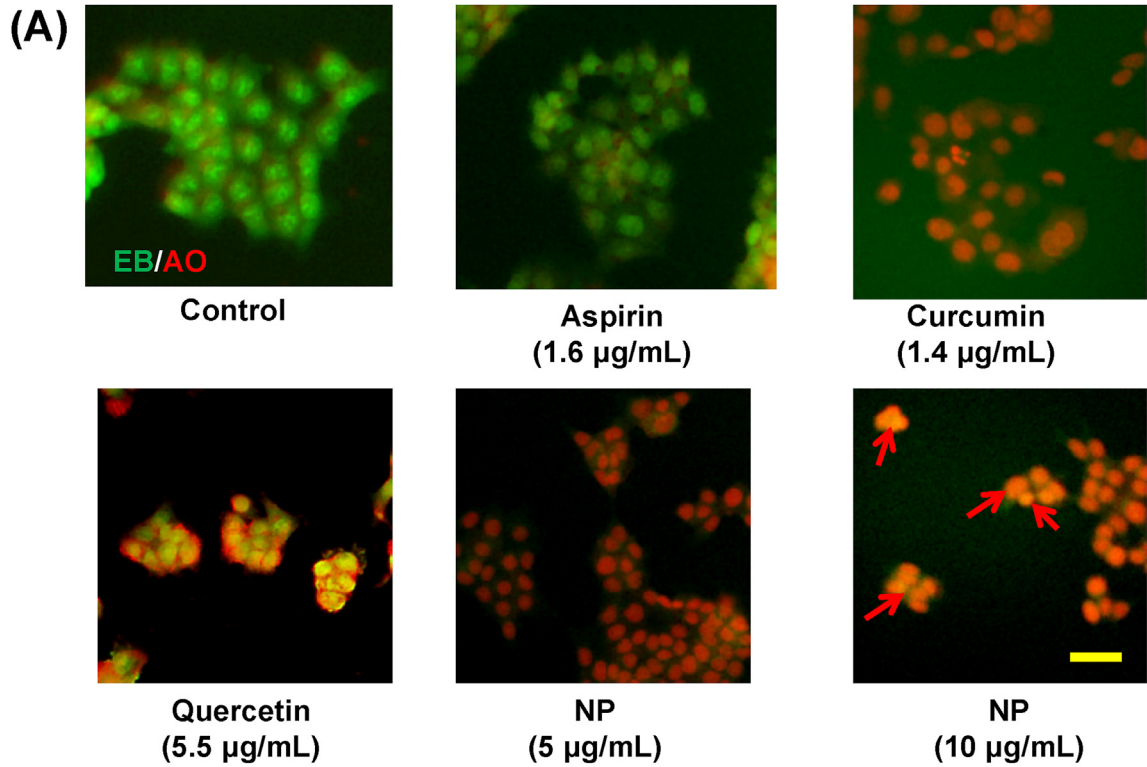


Fig. 8. (A) Morphological assays by EB/AO in cells to identify live, apoptotic and necrotic cells with the fluorescence of green, bright orange and red, respectively. The HCT-116 cells exposed to control and Aspirin (1.6 µg/mL) treated showed live cells (green), Curcumin (1.4 µg/mL), Quercetin (5.5 µg/mL), and CS-SHMP-CQA-NPs (5 and 10 µg/mL) treated cells showed apoptotic (bright orange) and necrotic cells (red). (Scale bar = 10 µm). (B) Percent (%) apoptotic (bright orange and red) cells in control, Aspirin (1.6 µg/mL), Curcumin (1.4 µg/mL), Quercetin (5.5 µg/mL), and CS-SHMP-CQA-NPs (5 and 10 µg/mL) treated HCT-116 cells by EB/AO staining. Data represented as mean ± SD of four image frames. [**p < 0.001 versus control, #p < 0.01 versus Quer and Asp, *p < 0.001 versus control and Cur].

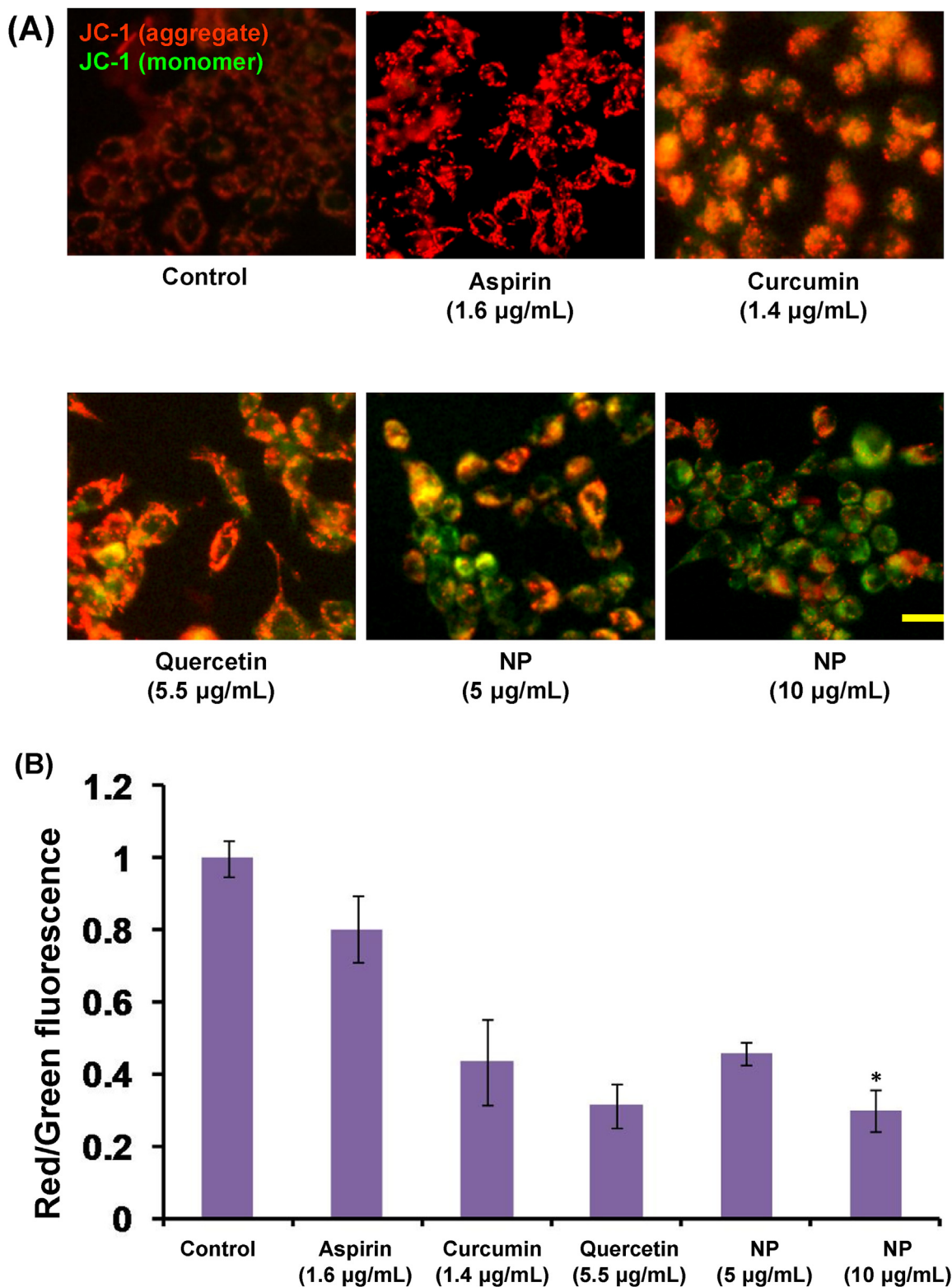


Fig. 9. (A) Mitochondrial membrane potential (MMP, $\Delta\psi_m$) by fluorescent dye JC-1 in control, free drugs and CS-SHMP-CQA-NPs (5 and 10 µg/mL) (JC-1 aggregates showed red color and green colors were from JC-1 monomers) (Scale bar = 10 µm). (B) Quantification of red to green JC-1 fluorescence intensity for drugs and CS-SHMP-CQA-NPs treated cells normalized to control. Data represented as mean \pm SD of four image frames [$*p < 0.01$ versus control and NP (5 µg/mL)].

the loss of mitochondrial membrane potential was calculated by NIH Image] software (USA) [20]. The percent (%) red fluorescence intensity revealed that ~1.9, ~1.7, ~1.5 and ~1.5-fold decrease in MMP in case of NP (10 µg/mL) compared to control, Asp (1.6 µg/mL), Cur

(1.4 µg/mL) and Quer (5.5 µg/mL) treated cells, respectively (Fig. 10B). Therefore, the combination of triplex chemopreventive agents in nanoparticles form significantly ($p < 0.05$) increased apoptosis in HCT-116 cells compared to individual drug treatment.

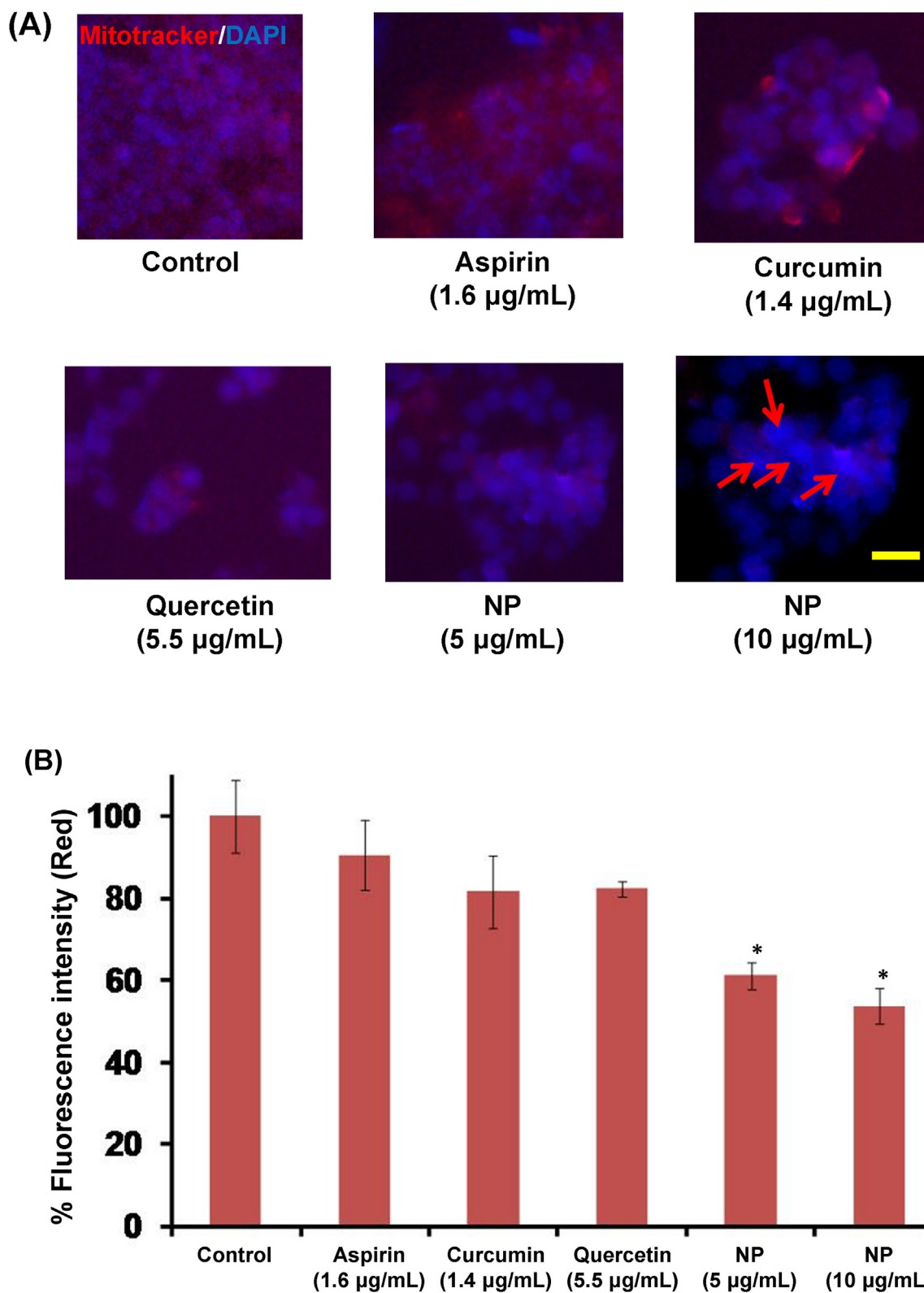


Fig. 10. (A) Mitotracker Red CMX-Ros/DAPI staining showed mitochondrial depolarization and DNA damage. (Scale bar = 10 µm). (B) Percentage (%) red fluorescence intensity of Mitotracker Red CMX-Ros/DAPI staining. Data represented as mean ± SD of four image frames [*p < 0.01 versus control].

4. Conclusions

A simple method was applied to entrap multiple chemotherapeutic agents in amphiphilic CS-SHMP polymer matrix, which was

prepared by means of electrostatic interactions. CS-SHMP polymer matrix not only holds multiple chemopreventive agents but also showed controlled drug release pattern, which was beneficial for efficient drug delivery. The formulation of Cur, Quer and Asp loaded

CS-SHMP-NPs significantly induced apoptosis, which was reflected by the decrease in MMP and increase in sub-G₁ cell population compared to the free chemopreventive agents in combination and two-drug-loaded nanoparticles. Moreover, three chemopreventive agents in NPs inhibited the progression of colon cancer cells (HCT-116) synergistically. Mucoadhesive properties of chitosan may enhance the absorption of chitosan; thus, improve the bioavailability and dosage of various drugs in the gastrointestinal tract in *in vivo* system. Furthermore, as three chemopreventive agents act through different pathways, anticipated synergistic effect would offer information about the clinical regimens for chemoprevention.

Conflict of interest statement

There are no conflicts of interest.

Acknowledgments

LR gratefully acknowledges the financial support provided by Young Scientist Grant, Department of Science and Technology (DST)-SERB (SB/FT/CS-034/2013), New Delhi, India (GAP-286; presently GAP-0206). MKP acknowledges ICMR, New Delhi for his fellowship (3/2/2/136/2012/NCD-III). Authors also wish to acknowledge Mr. Jay Shankar, Ms. Nidhi Arjaria, Dr. LKS Chouhan and Dr. PN Saxena for their support in TEM and SEM analysis at CSIR-IITR, Lucknow, India. The authors would like to thank Dr. K. C. Gupta (Department of BSBE and CESE, IIT, Kanpur) and Dr. Y. Shukla (CSIR-IITR, Lucknow), for their help and support for the work.

Appendix A. Supplementary data

Supplementary data related to this article can be found at <http://dx.doi.org/10.1016/j.bioactmat.2017.02.003>.

References

- [1] O. Stutman, Tumor development after 3-methylcholanthrene in immunologically deficient athymic-nude mice, *Science* 183 (1974) 534–536.
- [2] A. van Pel, T. Boon, Protection against a nonimmunogenic mouse leukemia by an immunogenic variant obtained by mutagenesis, *Proc. Natl. Acad. Sci. U. S. A.* 79 (1982) 4718–4722.
- [3] P. van der Bruggen, C. Traversari, P. Chomez, C. Lurquin, E. De Plaen, B. Van den Eynde, A. Knuth, T. Boon, A gene encoding an antigen recognized by cytolytic T lymphocytes on a human melanoma, *Science* 254 (1991) 1643–1647.
- [4] G. Willmsky, T. Blankenstein, Sporadic immunogenic tumors avoid destruction by inducing T-cell tolerance, *Nature* 437 (2005) 1411–1416.
- [5] A.B.M. Wilmink, Overview of the epidemiology of colorectal cancer, *Dis. Colon Rectum* 40 (1997) 483–493.
- [6] U.S. Cancer Statistics Working Group, United States Cancer Statistics: 1999–2005 Incidence and Mortality Web-based Report, U.S. Department of Health and Human Services, Centers for Disease Control and Prevention & National Cancer Institute, Atlanta, GA, 2009. Available at: www.cdc.gov/uscs (Accessed 21 October 2009).
- [7] F.A. Hagggar, R.P. Boushey, Colorectal cancer epidemiology: incidence, mortality, survival, and risk factors, *Clin. Colon Rectal Surg.* 22 (2009) 191–197.
- [8] P. Yager, T. Edwards, E. Fu, K. Helton, K. Nelson, M.R. Tam, B.H. Weigl, Microfluidic diagnostic technologies for global public health, *Nature* 442 (2006) 412–418.
- [9] W. Liu, X. Li, Y.S. Wong, W. Zheng, Y. Zhang, W. Cao, T. Chen, Selenium nanoparticles as a carrier of 5-Fluorouracil to achieve anticancer synergism, *ACS Nano* 6 (2012) 6578–6591.
- [10] M. Akhlu, C. Eng, The current landscape of locally advanced rectal cancer, *Nat. Rev. Clin. Oncol.* 8 (2011) 649–659.
- [11] D. Mukherjee, L.P. Rybak, K.E. Sheehan, T. Kaur, V. Ramkumar, S. Jajoo, S. Sheth, The design and screening of drugs to prevent acquired sensorineural hearing loss, *Expert Opin. Drug Discov.* 6 (2011) 491–505.
- [12] D. Lissa, L. Senovilla, S. Rello-Varona, I. Vitale, M. Michaud, F. Pietroccola, A. Boileve, F. Obrist, C. Bordenave, P. Garcia, J. Michels, M. Jemaà, O. Kepp, M. Castedo, G. Kroemer, Resveratrol and aspirin eliminate tetraploid cells for anticancer chemoprevention, *Proc. Natl. Acad. Sci. U. S. A.* 111 (2014) 3020–3025.
- [13] W.K. Hong, M.B. Sporn, Recent advances in chemoprevention of cancer, *Science* 278 (1997) 1073–1077.
- [14] G.D. Stoner, Foodstuffs for preventing cancer: the preclinical and clinical development of berries, *Cancer Prev. Res. (Phila)* 2 (2009) 187–194.
- [15] R. Rezaei-Sadabady, A. Eidi, N. Zarghami, A. Barzegar, Intracellular ROS protection efficiency and free radical-scavenging activity of quercetin and quercetin-encapsulated liposomes, *Artif. Cells Nanomed. Biotechnol.* 44 (2016) 128–134.
- [16] G. Biffi, D.A. Tuveson, Cancer: double trouble for tumours, *Nature* (2017), <http://dx.doi.org/10.1038/nature21117>.
- [17] C.S. Yang, H. Wang, B. Hu, Combination of chemopreventive agents in nanoparticles for cancer prevention, *Cancer Prev. Res. (Phila)* 6 (2013) 1011–1014.
- [18] B.B. Aggarwal, C. Sundaram, N. Malani, H. Ichikawa, Curcumin: the indian solid gold, in: *The Molecular Targets and Therapeutic Uses of Curcumin in Health and Disease*, Springer, 2007, pp. 1–75.
- [19] I. Erlund, Review of the flavonoids quercetin, hesperetin, and naringenin. Dietary sources, bioactivities, bioavailability and epidemiology, *Nutr. Res.* 24 (2004) 851–874.
- [20] D. Chopra, L. Ray, A. Dwivedi, S.K. Tiwari, J. Singh, K.P. Singh, H.N. Kushwaha, S. Jahan, A. Pandey, S.K. Gupta, R.K. Chaturvedi, A.B. Pant, R.S. Ray, K.C. Gupta, Photoprotective efficiency of PLGA-curcumin nanoparticles versus curcumin through the involvement of ERK/AKT pathway under ambient UV-R exposure in HaCaT cell line, *Biomaterials* 84 (2016) 25–41.
- [21] R. Wilken, M.S. Veena, M.B. Wang, E.S. Srivatsan, Curcumin: a review of anti-cancer properties and therapeutic activity in head and neck squamous cell carcinoma, *Mol. Cancer* 10 (2011) 12.
- [22] M.M. Yallapu, M. Jaggi, S. Chauhan, Curcumin nanoformulations: a future nanomedicine for cancer, *Drug Discov. Today* 17 (2012) 71–80.
- [23] M.H. Teiten, S. Eifes, M. Dicato, M. Diederich, Curcumin—the paradigm of a multi-target natural compound with applications in cancer prevention and treatment, *Toxins* 2 (2010) 128–162.
- [24] X.-A. Zhang, S. Zhang, Q. Yin, J. Zhang, Quercetin induces human colon cancer cells apoptosis by inhibiting the nuclear factor- κ B pathway, *Pharmacogn. Mag.* 11 (2015) 404–409.
- [25] W. Park, A.R. Amin, Z.G. Chen, D.M. Shin, New perspectives of curcumin in cancer prevention, *Cancer Prev. Res. (Phila)* 6 (2013) 387–400.
- [26] K. Wang, C. Zhang, J. Bao, X. Jia, Y. Liang, X. Wang, M. Chen, H. Su, P. Li, J.-B. Wan, C. He, Synergistic chemopreventive effects of curcumin and berberine on human breast cancer cells through induction of apoptosis and autophagic cell death, *Sci. Rep.* 6 (2016) 26064.
- [27] M.T. Huang, Y.R. Lou, W. Ma, H.L. Newmark, K.R. Reuhl, A.H. Conney, Inhibitory effects of dietary curcumin on forestomach, duodenal, and colon carcinogenesis in mice, *Cancer Res.* 54 (1994) 5841–5847.
- [28] J. Nautiyal, S.S. Kanwar, Y. Yu, A.P. N Majumdar, Combination of dasatinib and curcumin eliminates chemo-resistant colon cancer cells, *J. Mol. Signal.* 6 (2011) 7–18.
- [29] M.T. Huang, W. Ma, P. Yen, J.G. Xie, J. Han, K. Frenkel, D. Grunberger, A.H. Conney, Inhibitory effects of topical application of low doses of curcumin on 12-O-tetradecanoylphorbol-13-acetate-induced tumor promotion and oxidized DNA bases in mouse epidermis, *Carcinogenesis* 18 (1997) 83–88.
- [30] M.T. Huang, Z.Y. Wang, C.A. Georgiadis, J.D. Laskin, A.H. Conney, Inhibitory effects of curcumin on tumor initiation by benzo[a]pyrene and 7,12-dimethylbenzo[a]anthracene, *Carcinogenesis* 13 (1992) 2183–2186.
- [31] R. Hanif, L. Qiao, S.J. Shiff, B. Rigas, Curcumin, a natural plant phenolic food additive, inhibits cell proliferation and induces cell cycle changes in colon adenocarcinoma cell lines by a prostaglandin-independent pathway, *J. Lab. Clin. Med.* 130 (1997) 576–584.
- [32] D.P. Chauhan, Chemotherapeutic potential of curcumin for colorectal cancer, *Curr. Pharm. Des.* 8 (2002) 1695–1706.
- [33] R.E. Carroll, R.V. Benya1, D.K. Turgeon, S. Vared, M. Neuman, L. Rodriguez, M. Kakarala, P.M. Carpenter, C. McLaren, Phase IIa clinical trial of curcumin for the prevention of colorectal neoplasia, *Cancer Prev. Res. (Phila)* 4 (2011) 354–364.
- [34] B. Csokay, N. Prajda, G. Weber, E. Olah, Molecular mechanisms in the anti-proliferative action of quercetin, *Life Sci.* 60 (1997) 2157–2163.
- [35] M.F. Mouat, K. Kolli, R. Orlando, J.L. Hargrove, A. Grider, The effects of quercetin on SW480 human colon carcinoma cells: a proteomic study, *Nutr. J.* 4 (2005) 11–18.
- [36] J.-Y. Zhang, M.-T. Lin, M.-J. Zhou, T. Yi, Y.-N. Tang, S.-L. Tang, Z.-J. Yang, Z.-Z. Zhao, H.-B. Chen, Combinational treatment of curcumin and quercetin against gastric cancer MGC-803 Cells in vitro, *Molecules* 20 (2015) 11524–11534.
- [37] M.J. Thun, S.J. Henley, C. Patrono, Nonsteroidal anti-inflammatory drugs as anticancer agents: mechanistic, pharmacologic, and clinical issues, *J. Natl. Cancer Inst.* 94 (2002) 252–266.
- [38] C.V. Rao, B.S. Reddy, NSAIDs and chemoprevention, *Curr. Cancer Drug Targets* 4 (2004) 29–42.
- [39] W. Qiu, X. Wang, B. Leibowitz, H. Liu, N. Barker, H. Okada, N. Oue, W. Yasui, H. Clevers, R.E. Schoen, J. Yu, L. Zhang, Chemoprevention by nonsteroidal anti-inflammatory drugs eliminates oncogenic intestinal stem cells via SMAC-dependent apoptosis, *Proc. Natl. Acad. Sci. U. S. A.* 107 (2010) 20027–20032.
- [40] R.K. Pathak, S. Marrache, J.H. Choi, T.B. Berding, S. Dhar, The prodrug platin-A: simultaneous release of cisplatin and aspirin, *Angew. Chem. Int. Ed.* 53 (2014) 1–6.
- [41] M. Grilli, M. Pizzi, M. Memo, P. Spano, Neuroprotection by aspirin and sodium salicylate through blockade of NF- κ B activation, *Science* 274 (1996) 1383–1385.

- [42] M.J. Yin, Y. Yamamoto, R.B. Gaynor, The anti-inflammatory agents aspirin and salicylate inhibit the activity of I(κ)B kinase- β , *Nature* 396 (1998) 77–80.
- [43] M.J. Thun, S.J. Henley, C. Patrono, Nonsteroidal anti-inflammatory drugs as anticancer agents: mechanistic, pharmacologic, and clinical issues, *J. Natl. Cancer Inst.* 94 (2002) 252–266.
- [44] S. Temraz, D. Mukherji, A. Shamseddine, Potential targets for colorectal cancer prevention, *Int. J. Mol. Sci.* 14 (2013) 17279–17303.
- [45] R. Pai, T. Nakamura, W.S. Moon, A.S. Tarnawski, Prostaglandins promote colon cancer cell invasion; signaling by cross-talk between two distinct growth factor receptors, *FASEB J.* 17 (2003) 1640–1647.
- [46] X. Garcia-Albeniz, A.T. Chan, Aspirin for the prevention of colorectal cancer, *Best. Pract. Res. Clin. Gastroenterol.* 25 (2011) 461–464.
- [47] R.S. Sandler, Aspirin should not be promoted for colon cancer prevention: counterpoint, *Cancer Epidemiol. Biomarkers Prev.* 17 (2008) 1562–1563.
- [48] P. Anand, A.B. Kunnumakkara, R.A. Newman, B.B. Aggarwal, Bioavailability of curcumin: problems and promises, *Mol. Pharm.* 4 (2007) 807–818.
- [49] M.M. Yallapu, S. Khan, D.M. Maher, M.C. Ebeling, V. Sundram, N. Chauhan, A. Ganju, S. Balakrishna, B.K. Gupta, N. Zafar, Anti-cancer activity of curcumin loaded nanoparticles in prostate cancer, *Biomaterials* 35 (2014) 8635–8648.
- [50] H. Maeda, J. Wu, T. Sawa, Y. Matsumura, K. Hori, Tumor vascular permeability and the EPR effect in macromolecular therapeutics: a review, *J. Control Release* 65 (2000) 271–284.
- [51] Y. Matsumura, H. Maeda, A new concept for macromolecular therapeutics in cancer chemotherapy: mechanism of tumorotropic accumulation of proteins and the antitumor agent SMANCS, *Cancer Res.* 46 (1986) 6387–6392.
- [52] M.A. Ghaz-Jahani, F. Abbaspour-Aghdam, N. Anarjan, A. Berenjian, H. Jafarizadeh-Malmiri, Application of chitosan-based nanocarriers in tumor-targeted drug delivery, *Mol. Biotech.* 57 (2015) 201–218.
- [53] K.C. Gupta, F.H. Jabrail, Preparation and characterization of sodium hexameta phosphate cross-linked chitosan microspheres for controlled and sustained delivery of centchroman, *Int. J. Biol. Macromol.* 38 (2006) 272–283.
- [54] L. Zhou, X. Duan, S. Zeng, K. Men, X. Zhang, L. Yang, X. Li, Codelivery of SH-aspirin and curcumin by mPEG-PLGA nanoparticles enhanced antitumor activity by inducing mitochondrial apoptosis, *Int. J. Nanomedicine* 10 (2015) 5205–5218.
- [55] T.C. Chou, Drug combination studies and their synergy quantification using the Chou-Talalay method, *Cancer Res.* 70 (2010) 440–446.
- [56] D. Ribble, N.B. Goldstein, D.A. Norris, Y.G. Shellman, A simple technique for quantifying apoptosis in 96-well plates, *BMC Biotechnol.* 5 (2005) 12–19.
- [57] K. Deka, A. Singh, S. Chakraborty, R. Mukhopadhyay, S. Saha, Protein arginylation regulates cellular stress response by stabilizing HSP70 and HSP40 transcripts, *Cell Death Discov.* 2 (2016) e16074.
- [58] S.L. Lage, C.L. Buzzo, E.P. Amaral, K.C. Matteucci, L.M. Massis, M.Y. Icimoto, A.K. Carmona, M.R.D. Lima, M.M. Rodrigues, L.C.S. Ferreira, G.P. Amarante-Mendes, K.R. Bortoluci, Cytosolic flagellin-induced lysosomal pathway regulates inflammasome-dependent and -independent macrophage responses, *Proc. Natl. Acad. Sci. U. S. A.* 13 (2013) E3321–E3330.
- [59] U. Saeed, L. Durgadoss, R.K. Valli, D.C. Joshi, P.G. Joshi, V. Ravindranath, Knockdown of cytosolic glutaredoxin 1 leads to loss of mitochondrial membrane potential: implication in neurodegenerative diseases, *PLoS One* 3 (2008) e245927.
- [60] G. Casinelli, J. LaRosa, M. Sharma, E. Cherok, S. Banerjee, M. Branca, L. Edmunds, Y. Wang, S. Sims-Lucas, L. Churley, S. Kelly, M. Sun, D. Stolz, J.A. Graves, N-Myc overexpression increases cisplatin resistance in neuroblastoma via deregulation of mitochondrial dynamics, *Cell Death Discov.* 2 (2016) 16082.
- [61] K. Yoshida, M. Yoshioka, H. Okamura, S. Moriyama, K. Kawazoe, D. Grenier, D. Hinode, Preventive effect of Daiokanzoto (TJ-84) on 5-Fluorouracil-induced human gingival cell death through the inhibition of reactive oxygen species production, *PLoS One* 9 (2014) e112689.
- [62] Md. A. Rahim, S. Thatipamula, M.A. Hossain, Critical role of neuronal pentraxin 1 in mitochondria-mediated hypoxic-ischemic neuronal injury, *Neurobiol. Dis.* 50 (2013) 59–68.
- [63] S.-H. Zhang, F.-J. Gao, Z.-M. Sun, P. Xu, J.-Y. Chen, X.-H. Sun, J.-H. Wu, High pressure-induced mtDNA alterations in retinal ganglion cells and subsequent apoptosis, *Front. Cell Neurosci.* 10 (2016) 254.
- [64] S.T. Smiley, M. Reers, C. Mottola-Hartshorn, M. Lin, A. Chen, T.W. Smith, G.D. Steele, L.B. Chen, Intracellular heterogeneity in mitochondrial membrane potentials revealed by a J-aggregate-forming lipophilic cation JC-1, *Proc. Natl. Acad. Sci. U. S. A.* 88 (1991) 3671–3675.
- [65] G. MacDonald, L. Shi, C.V. Velde, J. Lieberman, A.H. Greenberg, Mitochondriadependent and-independent regulation of granzyme B-induced apoptosis, *J. Exp. Med.* 189 (1999) 131–144.
- [66] L. Ray, P. Kumar, K.C. Gupta, The activity against Ehrlich's ascites tumors of doxorubicin contained in self assembled, cell receptor targeted nanoparticle with simultaneous oral delivery of the green tea polyphenol epigallocatechin-3-gallate, *Biomaterials* 34 (2013) 3064–3076.
- [67] Y.S. Lakshmi, P. Kumar, G. Kishore, C. Bhaskar, A.K. Kondapi, Triple combination MPT vaginal microbicide using curcumin and efavirenz loaded lactoferrin nanoparticles, *Sci. Rep.* 6 (2016) 25479.
- [68] O. Kašpar, V. Tokárová, G.S. Nyanhongo, G. Gübitz, F. Štěpánek, Effect of cross-linking method on the activity of spray-dried chitosan microparticles with immobilized laccase, *Food Bioprod. Process.* 91 (2013) 525–533.
- [69] S.K. Hobbs, W.L. Monsky, F. Yuan, W.G. Roberts, L. Griffith, V.P. Torchilin, R.K. Jain, Regulation of transport pathways in tumor vessels: role of tumor type and microenvironment, *Proc. Natl. Acad. Sci. U. S. A.* 95 (1998) 4607–4612.
- [70] K.K. Upadhyay, A.K. Mishra, K. Chuttani, A. Kaul, C. Schatz, J.F. Le-Meins, A. Misra, S. Lecommandoux, The in vivo behavior and antitumor activity of doxorubicin-loaded poly(g-benzyl L-glutamate)-block-hyaluronan polymerosomes in Ehrlich ascites tumor-bearing BalB/c mice, *Nanomed. Nanotechnol.* 8 (2012) 71–80.
- [71] T. Dorai, B.B. Aggarwal, Role of chemopreventive agents in cancer therapy, *Cancer Lett.* 215 (2004) 129–140.
- [72] D.R. Green, J.C. Reed, Mitochondria and apoptosis, *Science* 281 (1998) 1309–1312.